Journal of Heat and Mass Transfer Research

Journal homepage: https://jhmtr.semnan.ac.ir

Semnan University

Research Article

Parameter Estimation in Mass Balance Model Applied in Fixed Bed Adsorption Using the Markov Chain Monte Carlo Method

Rhaisa Sousa Tavares [a], Camila Santana Dias [b], Carlos Henrique Rodrigues Moura [b], Emerson Cardoso Rodrigues [c], Bruno Marques Viegas [d], Emanuel Negrão Macêdo [c], Diego Cardoso Estumano [*,d]

[a] *Graduate Program in Process Engineering, Federal University of Pará, Pará, Brazil.*
[b] *Graduate Program in Natural Resource in the Amazon, Federal University of Pará, Pará, Brazil.*
[c] *Faculty of Chemical Engineering, Federal University of Pará, Pará, Brazil.*
[d] *Faculty of Biotechnology, Federal University of Pará, Pará, Brazil.*

PAPER INFO

Paper history:

Received: 2022-08-10
Revised: 2023-02-15
Accepted: 2023-02-21

Keywords:

Adsorption;
Breakthrough curve;
MCMC;
Parameter estimation;
Convergence analysis.

ABSTRACT

In this work, a mathematical model is adopted to predict the breakthrough curve in a fixed bed adsorption process, neglecting radial dispersion effects in the bed, with properties such as interstitial velocity and porosity being constant, linear adsorption kinetics and equilibrium relationship represented by the Langmuir isotherm. The resulting partial differential equation is numerically solved by the Method of Lines (MOL), while the Markov Chain Monte Carlo method is employed to estimate the model parameters, using simulated measures and a priori Gaussian probability distribution for the parameters, varying the mean and standard deviation. A convergence analysis was performed to look for numerical convergence between the number of nodes (N) used and the computational cost (CPU time) and it was observed that N = 100 obtained the lowest computational cost (less than 0.2 s). The estimated values of Peclet's number (Pe) and Langmuir's constant (KL) showed deviations of 7% and 0.01%, respectively, compared to their exact value which shows that the estimates were accurate, i.e., the parameters are close to the exact value. Also, the estimated values were within the credibility interval of 99 % established, which shows precise estimates. The information taken from these estimates has become of fundamental importance in predicting the behavior of the breakthrough curve at different points in the bed, showing that the MOL in combination with the MCMC are efficient tools in the direct and inverse analysis of models of breakthrough curves.

DOI: 10.22075/jhmtr.2023.28050.1389

1. Introduction

Pollution of water resources by the recalcitrant presence of emerging contaminants stimulates environmental concern about this topic and makes efforts aimed at remedying its negative effects on the environment relevant. In this sense, studies to develop effective methodologies for the treatment of these contaminants have been carried out around the world [1-9]

Among the already known methods that are effective for environmental remediation purposes are photocatalysis [10], membrane ultrafiltration

[*] *Corresponding Author: Diego Cardoso Estumano.*
Email: dcestumano@ufpa.br

[11] ,ozonation [12], photo-Fenton reaction [13] and ion exchange [14]. In this scenario, adsorption stands out as an attractive alternative for presenting relative simplicity of execution, low implementation cost compared to other approaches, and considerable level of effectiveness [15-17].

Adsorption can be performed in batch; however, this mode of operation is inappropriate when dealing with large-scale wastewater treatment [18-20]. Thus, for its industrial application, the use of fixed bed columns is suitable since they allow the continuous passage of effluents with a high load of pollutants through a column filled with adsorbent [18;21-22].

Before the elaboration of a project of an industrial scale fixed-bed column, a mathematical model capable of successfully representing the dynamics of experimentally obtained breakthrough curves is needed [23-24]. Many analytical models have been widely used to describe the breakthrough curves in fixed bed column adsorption systems [25-29].

Despite their importance, these models fail to identify mechanisms such as axial dispersion in the bed and mass transfer between phases. In addition, they need experimental curves for their parameters to be estimated, limiting the scope of the analysis to this specific curve [30-34].

To overcome the limitations of analytical models in representing breakthrough curves, several works have used more complex approaches in relation to the topic of adsorption in a fixed bed, some of which are highlighted in Table 1. In order to contribute to previous studies a model obtained from a mass balance for the fluid phase was used in this work, which is based on the conservation of mass in the system, kinetics, and conditions adsorption equilibrium[23].

The parameter estimation was performed from Bayesian inference perspective's to cover the effect that uncertainties intrinsic to the experimental execution would exert on the value found for the parameters. Since such effects can cause incompatibilities in the modeling by allowing physically improbable parameters to be obtained and, thus, affecting the design and operation of the process[35].

The Bayesian method of Markov Chain Monte Carlo (MCMC) was used in the estimation process. Simulated measurements were used to verify the elaborated code, and different levels of uncertainty were assigned to evaluate the effect produced on the results. The prior probability distribution, the one that contains previously available information about the analyzed system, was evaluated here by changes made to its characteristic metrics such as mean and standard deviation. The measurements that are usually obtained only at the exit of the bed were used to estimate information on the adsorptive process at other points in the column.

Table 1. Different approaches applied to the study of adsorption in a fixed bed column.

Breakthrough curve models	Equilibrium Isotherms	Kinetic	Solution Method	Parameter Estimation	Reference
Thomas Bohart-Adams Yan	-	-	Nonlinear adjustment	Origin Pro 8	[36]
Computational fluid dynamics (CFD)	Non-linear Langmuir	Linear Drive Force (LDF)	COMSOL Multiphysics	Empirical correlations	[24]
Thomas, Yoon-Nelson, Adams-Bohart and Wolbourska	-	-	Microsoft Excel's Solver Extension	Linear and Nonlinear Regression	[37]
Mass balance in fluid phase	Langmuir and BET	Linear Drive Force (LDF)	Runge-Kutta-Fehlberg Method	Minimization of an objective function using the downhill simplex optimization method	[38]
Logistic Model (Bohart-Adams, Yoon-Nelson and Thomas), Wolborska, Modified Dose-response, Clark, Gompertz and LogGompertz. Mass Transfer Model	Langmuir	Linear Drive Force (LDF)	Finite Elements	Comsol Multiphysics V5.4.	[34]
Hydrus-1D, Thomas, Yoon-Nelson and Bohart-Adams	General sorption model that, depending on the value of the parameters, may fall into the Langmuir, Freundlich or linear isotherm	-	Hydrus-1D	Levenberg-Marquardt and operational parameters by experiments	[39]

2. Direct Problem – Mass Balance

The representation of physical model is presented in Figure 1 and demonstrates in a simplified way an adsorption column with ascending feed of initial concentration C_0 and output current C.

The mass balance in a differential element of the bed was carried out assuming the following hypotheses: negligible radial dispersion, the significant variation was considered only in the axial direction, the solid/fluid interfaces establish a thermodynamic equilibrium state, porosity and interstitial velocity are constant [38].

$$\frac{\partial C(z,t)}{\partial t}+u_0\frac{\partial C(z,t)}{\partial z}= D_{ax}\frac{\partial^2 C(z,t)}{\partial z^2}-\frac{\rho_L}{\varepsilon_L}\frac{\partial q(z,t)}{\partial t} \quad 0<z<L,\ t>0 \tag{1.a}$$

$$\frac{\partial q(z,t)}{\partial t}=k_s\left(q^*(z,t)-q(z,t)\right) \quad 0<z<L,\ t>0 \tag{1.b}$$

Langmuir Isotherm:

$$q^*(z,t)=\frac{q_{\max}k_L C(z,t)}{1+k_L C(z,t)} \tag{1.c}$$

Initial conditions:

$$C(z,0)=0 \qquad 0<z<L,\quad t=0 \tag{1.d}$$

$$q(z,0)=0 \qquad 0<z<L,\quad t=0 \tag{1.e}$$

Boundary conditions:

$$-D_{ax}\frac{\partial C(z,t)}{\partial z}=u_0\left(C_o-C(z,t)\right) \quad z=0,\ t>0 \tag{1.f}$$

$$\frac{\partial C(z,t)}{\partial z}=0 \qquad z=L,\ t>0 \tag{1.g}$$

where u_0 is the fluid velocity, D_{ax} is the dispersion coefficient, ε_L is the bed void fraction, k_s is the kinetic constant, $q_{\max}$ is the maximum capacity of adsorption and k_L is the Langmuir parameter.

The dimensionless groups presented in Equation 2 were adopted; thus, the mass balance model in dimensionless form is shown in Equation 4.

$$\tau=\frac{t}{t_{ref}};\quad \eta=\frac{z}{L};\quad \theta=\frac{C}{C_0};\quad Q=\frac{q}{q_r};\quad Pe=\frac{u_0 L}{D_{ax}};\quad t_{ref}=\frac{L}{u_0} \tag{2.a-f}$$

$$\mathrm{K}_s=k_s t_{ref};\quad \mathrm{K}_L=k_L C_e;\quad q_r=\frac{C_0}{\rho_L};\quad Q^*=\frac{q^*}{q_r};\quad Q_{\max}=\frac{q_{\max}}{q_r} \tag{2.g-k}$$

where q_{max}, the maximum adsorption capacity in the column, is given by Equation (3):

$$q_{max}=\frac{C_0 Q}{1000W}\int_0^{t_r}\left(1-\frac{C}{C_0}\right)dt \tag{3}$$

where Q is the volumetric flow rate (cm^3/min) and W is the adsorbent mass (g).

$$\frac{\partial\theta(\eta,\tau)}{\partial\tau}+\frac{\partial\theta(\eta,\tau)}{\partial\eta}= \frac{1}{Pe}\frac{\partial^2\theta(\eta,\tau)}{\partial\eta^2}-\frac{1}{\varepsilon_L}\frac{\partial Q(\eta,\tau)}{\partial\tau} \quad 0<\eta<1,\ \tau>0 \tag{4.a}$$

$$\frac{\partial Q(\eta,\tau)}{\partial\tau}=\mathrm{K}_s\left(Q^*(\eta,\tau)-Q(\eta,\tau)\right) \quad 0<\eta<1,\ \tau>0 \tag{4.b}$$

$$Q^*(\eta,\tau)=\frac{Q_{\max}K_L\theta(\eta,\tau)}{1+K_L\theta(\eta,\tau)} \quad 0<\eta<1,\ \tau>0 \tag{4.c}$$

Initial conditions:

$$\theta(\eta,0)=0 \qquad 0<\eta<1,\ \tau=0 \tag{4.d}$$

$$Q(\eta,0)=0 \qquad 0<\eta<1,\ \tau=0 \tag{4.e}$$

Boundary conditions:

$$-\frac{\partial\theta(\eta,\tau)}{\partial\eta}=Pe\left(1-\theta(\eta,\tau)\right) \qquad \eta=0,\ \tau>0 \tag{4.f}$$

$$\frac{\partial\theta(\eta,\tau)}{\partial\eta}=0 \qquad \eta=1,\ \tau>0 \tag{4.g}$$

3. Metodology

3.1. Direct Model Solution – Methods Of Line

The numerical procedure used to solve the non-linear partial differential equation (PDE) was the method of lines. This method is used to solve the mass

balance model carried out in an adsorption column, to discretize the domain of the dependent variable $\theta(\eta,\tau)$ in space, transforming the obtained PDE into a system of time-continuous ordinary differential equations (ODEs) $\theta_i(\tau)$ [40].

The schematic representation shown in Figure 1 summarizes the discretization of the dimensionless domain in the range of $\eta=[0,1]$. In the method of lines, the domain $0<\eta<1$ is discretized into $\Delta\eta$ equal lengths, where $\Delta\eta=1/N-1$ and N is the number of nodes in the spatial domain. Therefore, N ODEs are developed by discretizing the governing PDE and boundary conditions [40].

Equations 4.a-c describe the dynamics that occur in the bed and correspond to the internal points of mesh in the domain interval. Equations 5.a-c show the discretized PDE.

$$\frac{d\theta_i}{d\tau}=-\frac{\theta_i-\theta_{i-1}}{\Delta\eta}+\frac{1}{Pe}\frac{\theta_{i+1}-2\theta_i+\theta_{i-1}}{\Delta\eta^2}-\frac{1}{\varepsilon_L}\frac{dQ_i}{d\tau} \tag{5.a}$$

$$\frac{dQ_i}{d\tau}=\mathrm{K}_s\left(Q_i^*-Q_i\right) \tag{5.b}$$

$$Q_i^*=\frac{Q_{\max}K_L\theta_i}{1+K_L\theta_i} \tag{5.c}$$

At $i=1$ and $\eta=0$ Equation 4.a takes the form described in Equation 5.d:

$$\frac{d\theta_1}{d\tau}=-\frac{\theta_1-\theta_0}{\Delta\eta}+\frac{1}{Pe}\frac{\theta_2-2\theta_1+\theta_0}{\Delta\eta^2}-\frac{1}{\varepsilon_L}\frac{dQ_1}{d\tau} \tag{5.d}$$

The boundary condition at the bed entrance described by Equation 4.f was used to determine θ_0, using the central difference on $i=1$, the arrangement as shown by Equation 5.

$$-\frac{\theta_1-\theta_0}{2\Delta\eta}=Pe\left(1-\theta_0\right)\therefore\ \theta_0=\frac{\theta_1+2\Delta\eta Pe}{1+2\Delta\eta Pe} \tag{5.e}$$

To determine θ_i at PDE in $i=N_i$ (Equation 5.f), the backward finite difference was applied to the boundary condition of Equation 4.g, which assumed the form shown in Equation 5.g.

$$\frac{d\theta_{Ni-1}}{d\tau}=-\frac{\theta_{Ni-1}-\theta_{Ni-2}}{\Delta\eta}+\frac{1}{Pe}\frac{\theta_{Ni}-2\theta_{Ni-1}+\theta_{Ni-2}}{\Delta\eta^2}-\frac{1}{\varepsilon_L}\frac{dQ_{Ni-1}}{d\tau} \tag{5.f}$$

$$\left.\frac{\partial\theta}{\partial\eta}\right|_{\eta=1}\Rightarrow 0\frac{\theta_N-\theta_{Ni-1}}{\Delta\eta}=0\ \ \therefore\ \ \theta_N=\theta_{Ni-1} \tag{5.g}$$

It is important to emphasize that the Method Of Lines is a methodology to obtain an approximate solution of the PDE given by the Equations (4.a-g). Therefore, the limitation of the method tends to be in the amount of precision needed to approximate the exact solution.

This accuracy is related to the number of grid points and available computing power. In this way, a convergence analysis becomes necessary to provide the computational power necessary to reach adequate precision to approximate the solution.

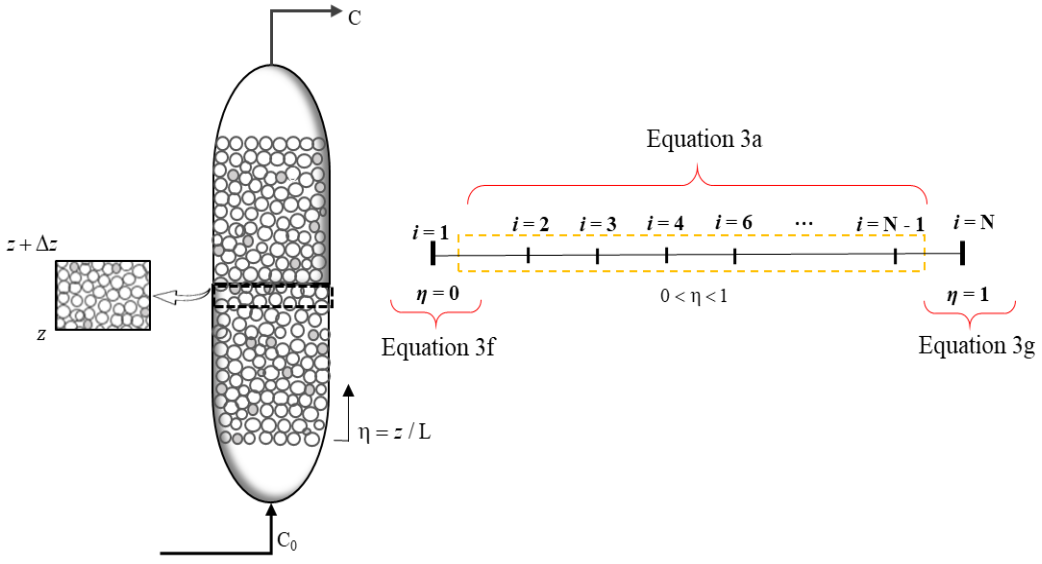

Figure 1. Model of an adsorption column and schematic representation of the domain discretized in the interval $\eta=[0,1]$

In this work, the algorithm used for convergence analysis is shown below:

1. Obtain $\boldsymbol{\theta}_1$ solving the direct problem using N nodes
2. Obtain $\boldsymbol{\theta}_2$ solving the direct problem using $N + \Delta N$ nodes
3. Calculate the tolerance, $tol = \max\left(\left|\boldsymbol{\theta}_1 - \boldsymbol{\theta}_2\right|\right)$. If $tol < tol_{SC}$ stop, otherwise do $\boldsymbol{\theta}_1 = \boldsymbol{\theta}_2$ and return to step 2.

where is the value of the dependent variable obtained for N nodes, $\boldsymbol{\theta}_2$ the value of the dependent variable obtained for $N + \Delta N$ nodes, N *is* the number of nodes in the mesh, *tol* is the tolerance and tol_{SC} is the initial defined tolerance.

3.2. Inverse Problem – Markov Chain Monte Carlo

In many cases, different prior probability densities can be assumed for the parameters and thus, it is impossible to obtain an analytical treatment for a posterior probability distribution. In this scenario, the Markov Chain Monte Carlo method, an iterative version of traditional Monte Carlo methods, is used to extract samples of all possible parameters so that posterior probability inference turns into sample inference [41-45].

The MCMC combines the properties of Monte Carlo and the Markov chain. The first is estimating the properties of distribution by examining random samples from the distribution. On the other hand, the second aims at the idea that a given sequential process generates random samples, where each random selection is used as a step to develop the next one. A particular property is that, although each new choice depends on the previous one, new samples do not rely on any instance before the last one.

In the present work, the Metropolis-Hastings algorithm is used to estimate the parameters of the mathematical model of the breakthrough curve[41;46-50], which following the following steps:

1. Initially, set an initial parameter value for the first iteration of the chain, $\mathbf{P}^1$. Then, draw a candidate value $\mathbf{P}^*$ from an auxiliary distribution q ($\mathbf{P}^* \mid \mathbf{P}^i$). In the present work, the auxiliary distribution adopted is a Gaussian distribution in the following form:

$$\mathbf{P}^* = \mathbf{P}^i\left(1 + \mathbf{w}\xi\right) \tag{6}$$

where ξ is a random variable $N(0,1)$ and w is the search step.

2. Compute the probability of acceptance $\alpha\left(\boldsymbol{P}^{(i)} \middle| \boldsymbol{P}^*\right)$ of the candidate value given by:

$$\alpha\left(\boldsymbol{P}^{(i)} \middle| \boldsymbol{P}^*\right) = \min\left[1, \frac{\pi\left(\mathbf{P}^* \middle| \mathbf{Y}\right) q\left(\mathbf{P}^{(i)} \middle| \mathbf{P}^*\right)}{\pi\left(\mathbf{P}^{(i)} \middle| \mathbf{Y}\right) q\left(\mathbf{P}^* \middle| \mathbf{P}^{(i)}\right)}\right] \tag{7}$$

3. Generate a random number u from a uniform distribution U(0,1);
4. If $u \leq \alpha\left(\boldsymbol{P}^i \middle| \boldsymbol{P}^*\right)$, accept the new $\boldsymbol{P}^{(i+1)} = \boldsymbol{P}^*$ value. Otherwise, $\boldsymbol{P}^{(i-1)} = \boldsymbol{P}^{(i-1)}$.
5. Return to step 1.

A flowchart of the Metropolis-Hastings algorithm is illustrated in Figure 2 below.

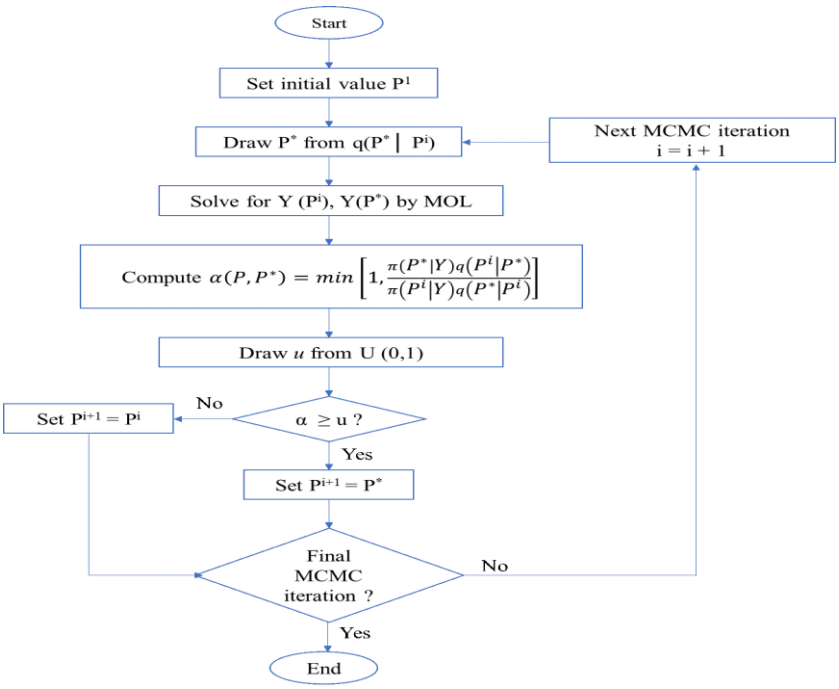

Figure 2. Sequential flowchart of the MCMC method using Metroplis-Hastings

In this work, simulated measures are used to carry out parameter estimates. Such measures are generated by adding noise, υ, so the measures by Equation (8):

$$\boldsymbol{\theta}^{meas}\left(1,\tau\right)=\boldsymbol{\theta}^{exact}\left(1,\tau\right)+\boldsymbol{\nu} \quad (8)$$

where $\boldsymbol{\theta}^{exact}\left(1,\tau\right)$ is the solution of the direct problems with knowing reference parameters and $\boldsymbol{\nu}=N\left(\mathbf{0},\ \boldsymbol{\sigma}_{meas}\right)$.

4. Results

The numerical tests carried out concerned the direct model's evaluation (presented in section 2) using the technique shown in section 3 to solve the inverse problem of parameter estimation involved in the adsorption phenomenon in a fixed bed column

The system of ordinary differential equations originated from the discretization of the partial differential equation and was solved by the *ode15s* function of the Matlab R2021a software. The same software programmed code for the Metropolis-Hastings algorithm.

The mesh convergence analysis is performed to verify the number of nodes (N_i) sufficient for model discretization when applying the method of lines and reaching a satisfactory convergence.

The number of nodes in the discretized domain varied, and how this variation influenced the computational time was observed. The relevance of this analysis for this work aim at the need that the MCMC method must solve the direct model several times (10.000 states of Markov Chain), therefore defining the number of nodes and the desirable computational cost to obtain precision in the solution becomes desirable.

Simulated measurements were used to apply the estimates of the parameters of the analyzed model. The prior probability distribution of the parameters was adopted as Gaussian, and its influence and the influence of the acquisition frequency of measurements are evaluated. The simulations were performed using as a reference for the parameters the following values: Pe = 10.00, Ks = 1.00, Q_{max} = 7.00, K_L = 1.00 and ε = 0.40. The choice of these parameters was to simulate a breakthrough without numerical instabilities, since the Peclet number (Pe) can be important to characterize the transport of solutes by advective or diffusive means, the numerical stability depends on the number of Pe. If they reach some critical limits the numerical solution begins oscillating in space and time.

The parameters Q_{max}, K_s can be calculated, and the porosity ε can be obtained experimentally. In this sense, the parameters estimated here were *Pe* because they included operational and diffusivity information, and K_L referring to the Langmuir isotherm.

4.1. Convergence Analysis

Figure 3 presents the results of the convergence analysis performed. It has been found that increasing the number of nodes increases the computational cost

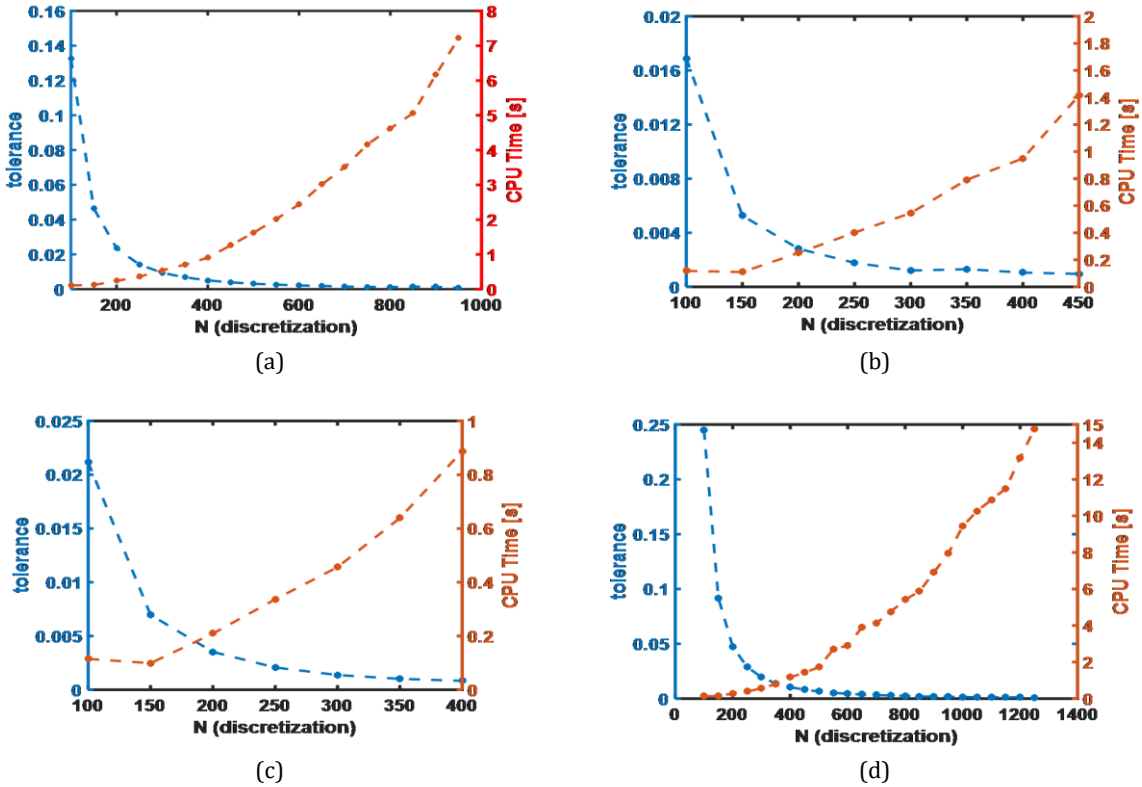

Figure 3. Convergence analysis regarding Q_{max} and ε were kept constant in 7.00 and 0.40, respectively. (a) Pe = 10.00 ; K_L = 1.00, (b) Pe = 10.00 ; K_L = 3.00, (c) Pe = 2.00 ; K_L = 1.00 e (d) Pe = 20.00 ; K_L = 1.00.

4.2. Prior Mean Analysis

The prior probability distribution of the parameters contains the information previously known. In this sense, variations in the mean of the prior probability distribution of the parameters, shown in Table 1, were performed to evaluate whether the estimated values would approach the exact value when the mean value of this distribution is changed.

The graph of the prior probability distribution function for these case studies is shown in Figure 4. It is possible to notice the displacement of the mean of the probability density distributions of the parameters Pe and K_L for each case concerning the value adopted as reference (green line).

Figure 5 shows the estimation result for case studies 1 and 5(see Table 2). It is observed that the prior distribution mean is far from the exact value. After the estimation process, the result shown by the posterior probability distribution converges to a determined region close to the reference, suggesting that despite the displacement carried out in the prior mean, adequate information regions to select candidate parameters could be reached, demonstrating the robustness of the MCMC method.

Table 2 shows the results of the estimates in all cases in which the influence of the displacement of the mean on the prior probability distribution is evaluated. It was possible to observe that there was precision for all cases since the estimated parameters are within the 95% credibility interval and accuracy since the estimates are close to the exact value of the parameters. It is also found that the deviations from the parameters' estimates were low and had a low level of uncertainty.

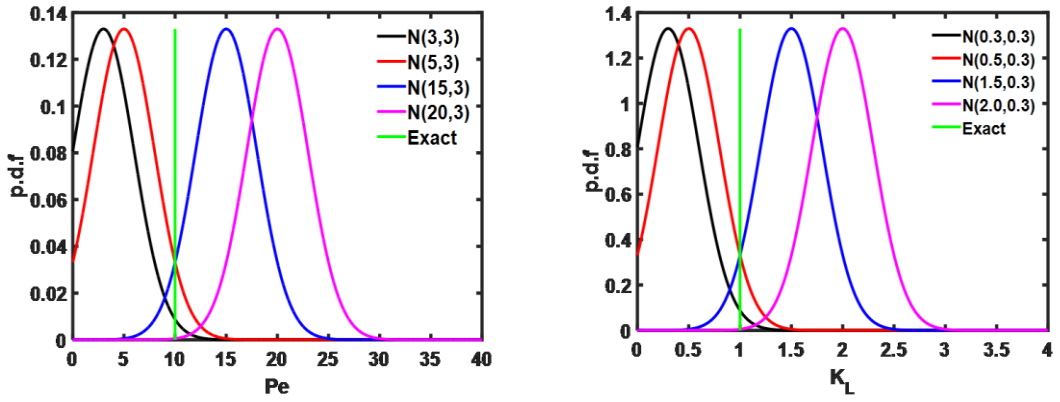

(a) (b)

Figure 4. Prior probability distribution function (pdf) evaluating the influence of the mean for the parameters: (a) Pe e (b) K_L.

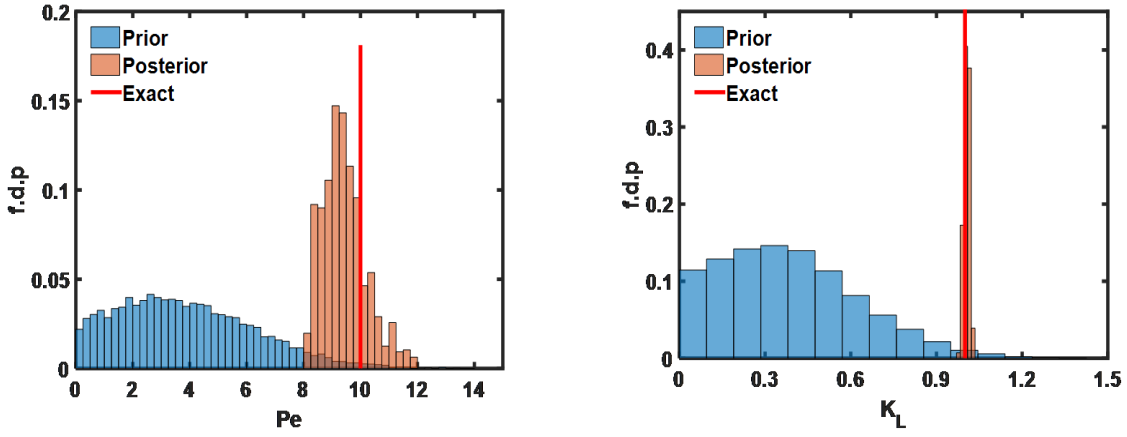

(a) (b)

Figure 5. Prior and posterior probability distribution function evaluating the influence of the mean displacement on the parameters' prior: (a) Pe e (b) K_L

Table 2. Influence of the mean on the prior probability distribution.

Caso	Parameter	Exact	$\pi_{prior}(\mathbf{P})$	$\pi_{posterior}(\mathbf{P})$
1	Pe	10.00	N(3, 3)	9.84 (9.39;10.38)
2		10.00	N(5, 3)	9.79 (9.37;10.18)
3		10.00	N(15, 3)	10.02 (9.31;10.66)
4		10.00	N(20, 3)	9.39 (8.96;9.74)
5	K_L	1.00	N(0.3, 0.3)	1.00 (0.99;1.01)
6		1.00	N(0.5, 0.3)	1.00 (0.99;1.02)
7		1.00	N(1.5, 0.3)	1.00 (0.99;1.02)
8		1.00	N(2.0, 0.3)	1.01 (0.99;1.02)

4.3. Prior Standard Deviation Analysis

In addition to analyzing the influence of the mean, another critical assessment is to observe the effect that the variation in the standard deviation can have on the estimates since high standard deviation values can lead to uninformative priors. Even though they lead to own posteriors, poorly informative priors can generate a certain instability when posterior is obtained numerically [51].

Figure 6 shows the influence of different standard deviation values on the prior probability distribution function of the parameters. It is possible to observe that the search for candidate parameters falls within a reduced range of values, whereas for more significant deviations, this range is extended.

Table 3 shows the results (mean and credibility interval 99%) obtained for the estimates by varying the standard deviation of the prior probability distribution of the parameters. It is observed that the increase in deviation decreases the accuracy of the estimates since the estimated values are far from the exact value.

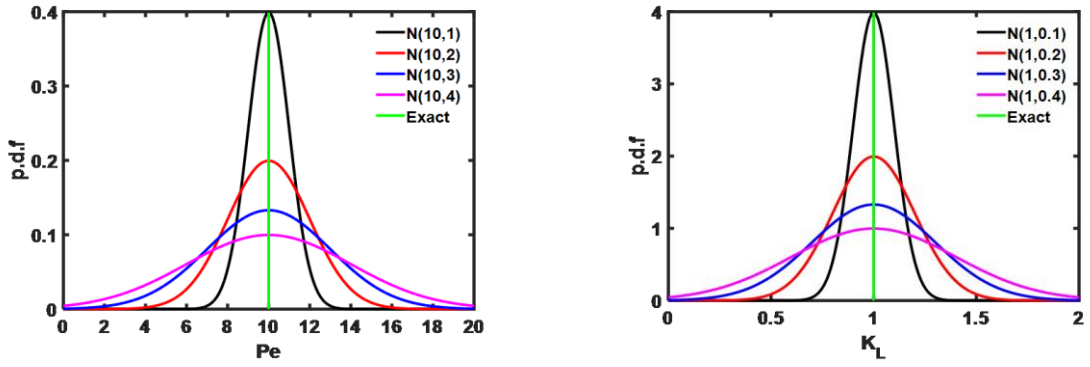

Figure 6. Prior probability distribution function evaluating the influence of standard deviation on the prior for parameters: (a) Pe e (b) K_L.

Table 3. Influence of the standard deviation on the prior probability distribution.

Parameter	Exact	$\pi_{prior}(\mathbf{P})$	$\pi_{posterior}(\mathbf{P})$
Pe	10.00	N (10,1)	10.05 (9.47; 10.68)
	10.00	N (10,2)	9.34 (8.87; 10.10)
	10.00	N (10,3)	9.37 (8.65; 9.94)
	10.00	N (10,4)	9.33 (8.95; 9.70)
K_L	1.00	N(1,0.1)	1.00 (0.99; 1.01)
	1.00	N(1,0.2)	1.01 (0.99; 1.02)
	1.00	N(1,0.3)	1.01 (0.99; 1.02)
	1.00	N(1,0.4)	1.01 (1.00; 1.03)

4.4. Acquisition Frequency Of Measurements

Figure 7 seeks to represent the acquisition frequency of measurements, dτ, and how uncertainties associated, σ_{meas}, influence the data dispersion. As shown in Figure 7a-d, it is possible to observe that as dτ increases, the number of measurements obtained decrease. On the other hand, measurements are placed close to the breakthrough curve at low values attributed to uncertainty, such as 1%. Higher values of σ_{meas} were used to represent more realistic scenarios and interfered in the increase of dispersion around the reference curve, as observed in Figure 7e-g.

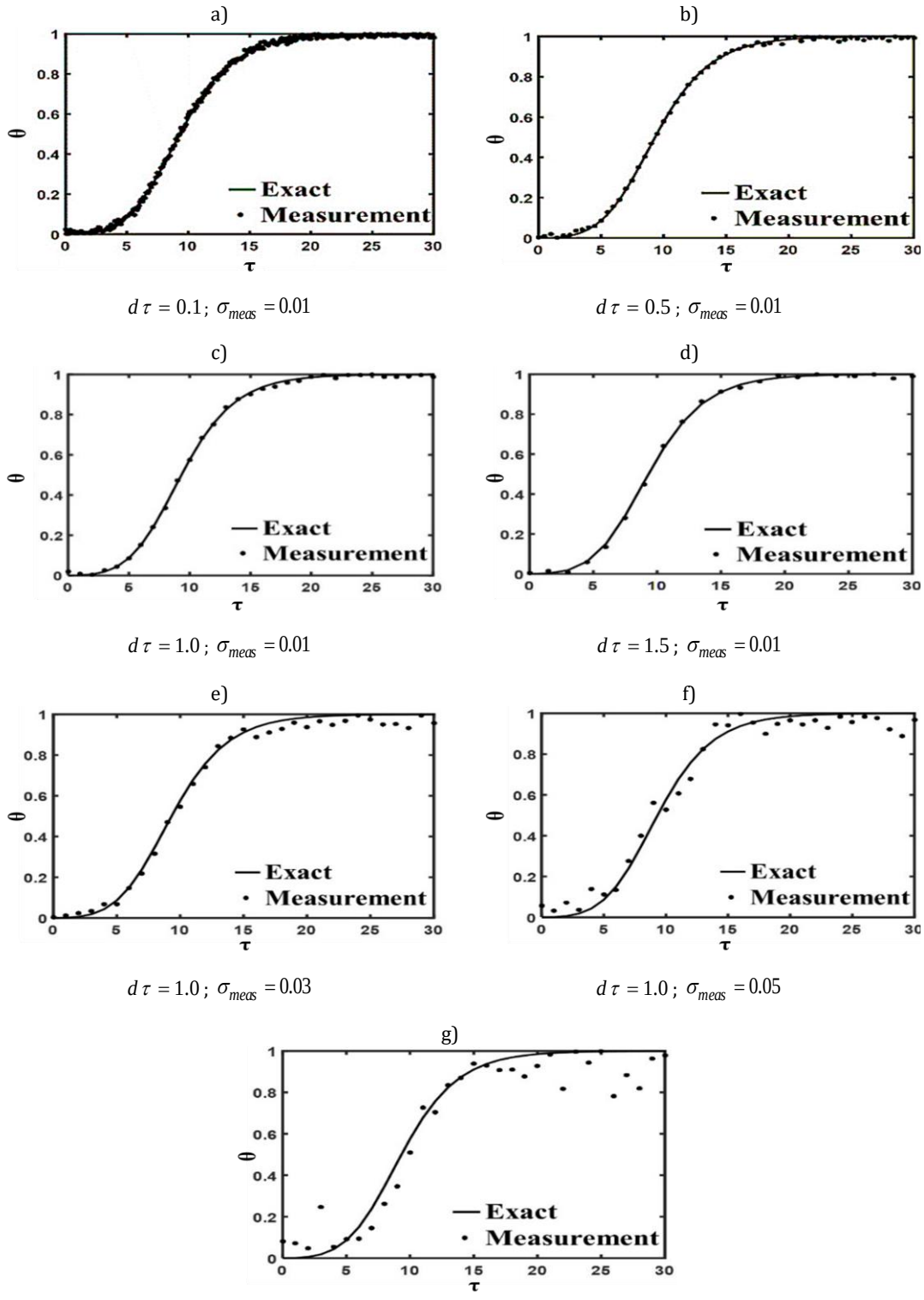

Figure 7. Acquisition frequency of measurements and influence of the increase in uncertainty.

4.5. Breakthorough Curve Estimation

The parameters estimated from the use of the MCMC Bayesian method allowed that measurements obtained in the output current could offer the possibility of predicting curves that form at different points along the column. In this work, the analyzed points were close to the inlet θ = 0.25, in the middle θ = 0.5 and at the exit of the column θ = 1. The results presented in Figure 8 showed the dynamics of the advance of the adsorptive phenomenon.

Figure 8a), c) and e) show the comparison between the exact solution of the model (black line) and the one obtained from the prior probability distribution of the parameters (solid blue line).

Figure 8b), d) and f) show the results for the exact solution of the model (black line) and the one obtained from the a posteriori probability distribution of the estimates made with the MCMC method (solid blue line). You can see that the exact and estimated curves overlap and remain within a 95% confidence interval (dashed blue line). It is evident that an excellent agreement was achieved between the estimated and exact measurements.

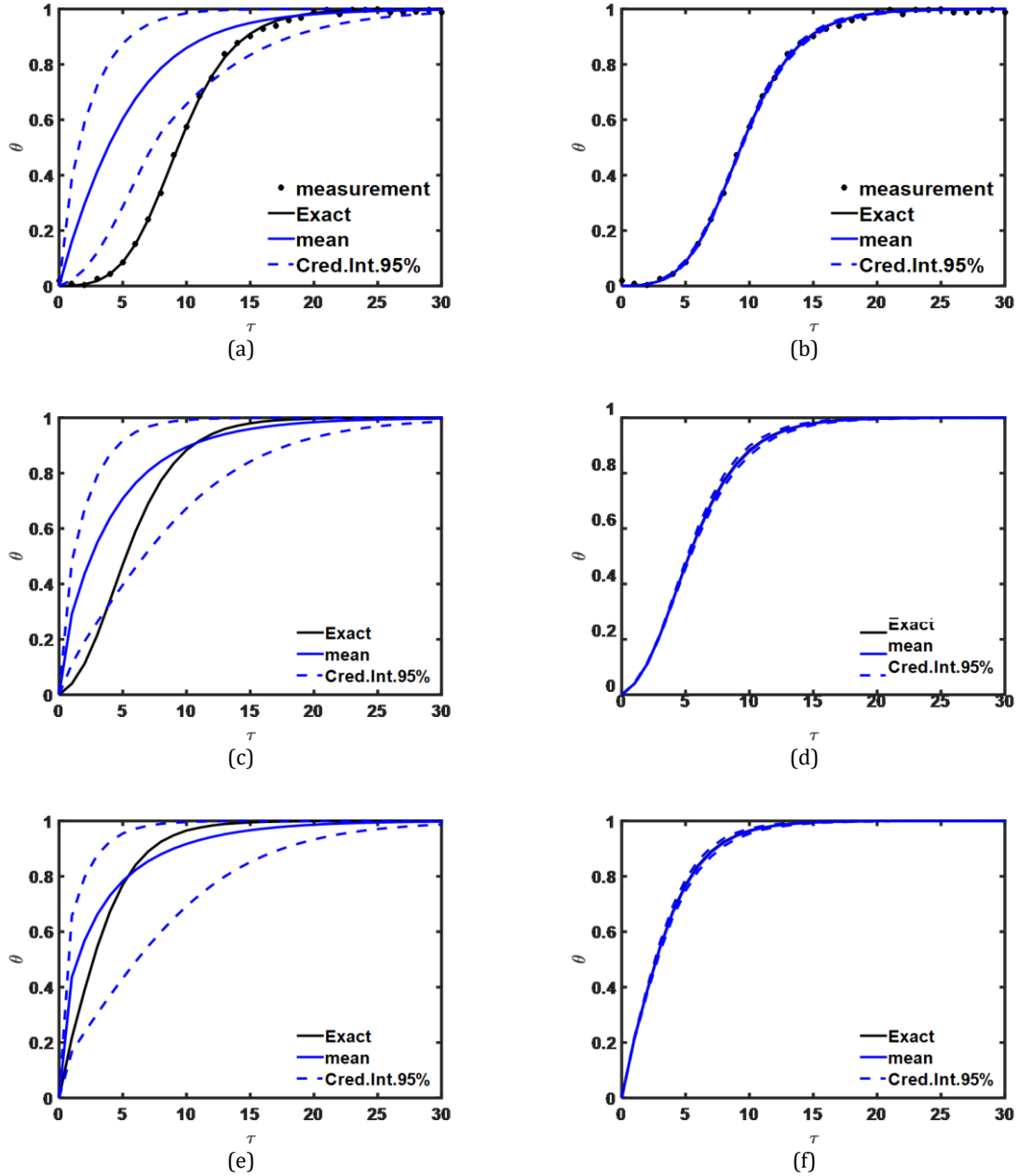

Figure 8. Estimation of the breakthrough curve at different points in the fixed bed column. a) $\theta(1.00,\tau)$ from $\pi_{prior}(\mathbf{P})$, b) $\theta(1.00,\tau)$ from $\pi_{posterior}(\mathbf{P})$, c) $\theta(0.50,\tau)$ from $\pi_{prior}(\mathbf{P})$, d) $\theta(0.50,\tau)$ from $\pi_{posterior}(\mathbf{P})$, e) $\theta(0.25,\tau)$ from $\pi_{prior}(\mathbf{P})$ f) $\theta(0.25,\tau)$ from $\pi_{posterior}(\mathbf{P})$

Conclusion

The parameters estimation of the mathematical model of the adsorption of a chemical species in a fixed bed column was performed using the Markov Chain Monte Carlo method. In addition, simulated measurements generated from Gaussian noises were used to verify the developed algorithm.

The obtained model is solved by the Method of Lines, and a mesh convergence study was carried out to determine a sufficient value of discretization. A high tolerance value demands many discretization, which is not desirable since this increases the computational cost and causes numerical and approximation errors to occur. However, in the present work, the increase in computational cost was not significant.

The estimate analysis explored two scenarios: the influence of the mean and standard deviation on the prior probability distribution of the Peclet number, Pe, and the Langmuir isotherm constant, K_L. In these scenarios, we observed that even changing the prior distribution of the parameters, the posterior distribution samples converge to values close to exact. Thus, the estimated results were satisfactory, and there was both precision and accuracy in the inferences.

From the Bayesian inference, it was possible to use the information at a certain point in the column and thus obtain estimates with considerable precision in other places of interest where measurements were not available. The simulated scenario also allowed the observation of the influence of experimental uncertainties in obtaining measurements, showing that they tend to present greater dispersion the greater the uncertainties associated with their acquisition.

Thus, from the results presented, it is shown that the application of the Bayesian technique of MCMC is robust and presents itself as an excellent tool to understand the dynamics of the fixed bed adsorption process and other mass transfer processes.

Nomenclature

C	Adsorbate concentration at bed outlet, (mg.L^{-1})
q	Adsorbate concentration at solid phase, (mg.g^{-1})
u_0	Interstitial velocity, (cm.min^{-1})
D_{ax}	Axial dispersion coefficient, (cm^2.min^{-1})
k_L	Langmuir constant, (L.mg^{-1})
$q_{\max}$	Maximum adsorption capacity, (mg.g^{-1})
k_s	Global mass transfer coefficient, (min^{-1})
q^*	Equilibrium concentration in the solid phase, (mg.g^{-1})
ε_L	Porosity
t	Time, (min)
ρ_L	Bed density, (g.L^{-1})
θ	Dimensionless concentration of adsorbate at bed outlet
Q	Dimensionless concentration of adsorbate in the solid phase
Pe	Peclet number
K_L	Dimensionless Langmuir Constant
$Q_{\max}$	Dimensionless maximum adsorption capacity
K_s	Dimensionless global mass transfer coefficient
η	Dimensionless length
Q^*	Dimensionless equilibrium concentration in the solid phase
τ	Dimensionless time

Conflicts of Interest

The authors declare that have no conflict of interest regarding the publication of this article.

References

[1] PEREIRA, A. M., SILVA, L. J., LARANJEIRO, C. S., MEISEL, L. M., LINO, C. M., PENA, A. Human pharmaceuticals in Portuguese rivers: The impact of water scarcity in the environmental risk. *Science of the Total Environment*, v. 609, p. 1182-1191, 2017.

[2] SOUZA, F. S., SILVA, V. V., JANK, L., ROSIN, C. K., HAINZENREDER, L., ARENZON, A., PIZZOLATO, T., FERIS, L.A., Determination of pharmaceutical compounds in hospital wastewater and their elimination by advanced oxidation processes. *Journal of environmental science and health part a-toxic/hazardous substances & environmental Engineering*, p. 1-9, 2017.

[3] SOUZA, F.S., SILVA, V.V., ROSIN, C. K., HAINZENREDER, L., ARENZON, A. FÉRIS, L.A., Comparison of different advanced oxidation processes for the removal of amoxicillin in aqueous solution. *Environmental Technology*, 39:5, 549-557, 2018.

[4] ZOUMPOULI, G. A., SIQUEIRA SOUZA, F., PETRIE, B., FÉRIS, L. A., KASPRZYK-HORDERN, B., WENK, J., Simultaneous ozonation of 90 organic micropollutants including illicit drugs and their metabolites in different water matrices. *Environmental Science: Water Research and Technology*, *6*(9), 2020.

[5] DÁVILA, I. V. J., HÜBNER, J. V. M., NUNES, K. G. P., & FÉRIS, L. A., Caffeine Removal by Adsorption: Kinetics, Equilibrium Thermodynamic and Regeneration Studies. *The Journal of Solid Waste*

Technology and Management, *47*(1), 95-103, 2021. https://doi.org/10.5276/JSWTM/2021.95.

[6] ROSSET, M., SFREDDO, L. W., PEREZ-LOPEZ, O. W., & FÉRIS, L. A, Effect of concentration in the equilibrium and kinetics of adsorption of acetylsalicylic acid on ZnAl layered double hydroxide. *Journal of Environmental Chemical Engineering*, *8*(4), 103991, 2020. https://doi.org/10.1016/j.jece.2020.103991.

[7] COSTA, L. R. D. C., FÉRIS, L. A., Use of functionalized adsorbents for tetracycline removal in wastewater: adsorption mechanism and comparison with activated carbon. *Journal of Environmental Science and Health, Part A*, *55*(14), 1604-1614, 2020.

[8] HARO, N. K., DÁVILA, I. V. J., NUNES, K. G. P., DE FRANCO, M. A. E., MARCILIO, N. R., & FÉRIS, L. A.,Kinetic, equilibrium and thermodynamic studies of the adsorption of paracetamol in activated carbon in batch model and fixed-bed column. *Applied Water Science*, *11*(2), 2021. https://doi.org/10.1007/s13201-020-01346-5.

[9] SANTOS, T. C.S., ALMEIDA, A. C. M., do Rosario Pinheiro, D., COSTA, C. M. L., ESTUMANO, D. C., & da Paixao Ribeiro, N. F. (2020). Synthesis and characterization of colourful aluminates based on nickel and zinc. *Journal of Alloys and Compounds*, *815*, 152477.

[10] BARROCAS, B., NEVES, M. C., OLIVEIRA, M. C., MONTEIRO, O. C. Enhanced photocatalytic degradation of psychoactive substances using amine-modified elongated titanate nanostructures. *Environmental Science: Nano*, v. 5, n. 2, p. 350-361, 2018. https://doi.org/10.1039/C7EN00882A.

[11] KIM, S., CHU, K. H., AL-HAMADANI, Y. A., PARK, C. M., JANG, M., KIM, D. H., YOON, Y. Removal of contaminants of emerging concern by membranes in water and wastewater: a review. *Chemical Engineering Journal*, v. 335, p. 896-914, 2018. https://doi.org/10.1016/j.cej.2017.11.044.

[12] LIU, C., LI, P., TANG, X., KORSHIN, G. V. Ozonation effects on emerging micropollutants and effluent organic matter in wastewater: characterization using changes of three-dimensional HP-SEC and EEM fluorescence data. *Environmental Science and Pollution Research*, v. 23, n. 20, p. 20567-20579, 2016. https://doi.org/10.1007/s11356-016-7287-8.

[13] OLLER, I.; MALATO, S. Photo-Fenton applied to the removal of pharmaceutical and other pollutants of emerging concern. *Current Opinion in Green and Sustainable Chemistry*, p. 100458, 2021. https://doi.org/10.1016/j.cogsc.2021.100458.

[14] HU, Y.; BOYER, T. H. Removal of multiple drinking water contaminants by combined ion exchange resin in a completely mixed flow reactor. *Journal of Water Supply: Research and Technology-Aqua*, v. 67, n. 7, p. 659-672, 2018. https://doi.org/10.2166/aqua.2018.101.

[15] LV, Y., LIANG, Z., LI, Y., CHEN, Y., LIU, K., YANG, G., LIU, M. Efficient adsorption of diclofenac sodium in water by a novel functionalized cellulose aerogel. *Environmental Research*, v. 194, p. 110652, 2021.

[16] TATARCHUK, T., MYSLIN, M., LAPCHUK, I., SHYICHUK, A., MURTHY, A. P., GARGULA, R., PĘDZIWIATR, A. T. Magnesium-zinc ferrites as magnetic adsorbents for Cr (VI) and Ni (II) ions removal: cation distribution and antistructure modeling. *Chemosphere*, v. 270, p. 129414, 2021. https://doi.org/10.1016/j.chemosphere.2020.129414.

[17] SHARAFEE, M. S., AZHA, S. F., BADAWI, M., BONILLA-PETRICIOLET, A. Performance and interactions of diclofenac adsorption using Alginate/Carbon-based Films: Experimental investigation and statistical physics modelling. *Chemical Engineering Journal*, p. 131929, 2021. https://doi.org/10.1016/j.cej.2021.131929.

[18] RUTHVEN, D. M. *Principles of adsorption and adsorption processes*. John Wiley & Sons, 1984.

[19] TIEN, C. *Introduction to adsorption: Basics, analysis, and applications*. Elsevier, 2018. https://doi.org/10.1016/C2018-0-00297-2.

[20] DOTTO, G.L., MCKAY, G. Current scenario and challenges in adsorption for water treatment, *Journal of Environmental Chemical Engineering*, 8(4), 103988, 2020. https://doi.org/10.1016/j.jece.2020.103988.

[21] AKSU, Z., GÖNEN, F., Binary biosorption of phenol and chromium (VI) onto immobilized activated sludge in a packed bed: prediction of kinetic parameters and breakthrough curves, *Separation and Purification Technology*, 49(3), 205-216, 2006.

[22] PATEL, H., Fixed-bed column adsorption study: a comprehensive review, *Applied Water Science*, 9(3), 1-17, 2019. https://doi.org/10.1007/s13201-019-0927-7

[23] XU, Z., CAI, J. G., PAN,B.C., Mathematically modeling fixed-bed adsorption in aqueous systems, *Journal of Zhejiang University SCIENCE A*, 14(3), 155-176, 2013.

[24] VERA, M., JUELA, D. M., CRUZAT, C., & VANEGAS, E., Modeling and computational fluid dynamic simulation of acetaminophen adsorption using sugarcane bagasse, *Journal of Environmental Chemical Engineering*, 9(2), 105056, 2021.

[25] THOMAS, H. C. The kinetics of fixed-bed ion exchange. *Ion Exchange, FC Nachod, ed*, 29,1949.

[26] YOON, Y. H., NELSON, J. H., Application of gas adsorption kinetics I. A theoretical model for respirator cartridge service life, *American Industrial Hygiene Association Journal*, *45*(8), 509-516, 1984.

[27] CLARK, R. M., Evaluating the cost and performance of field-scale granular activated carbon systems. *Environmental science & technology*, *21*(6), 573-580, 1987.

[28] WOLBORSKA, A., Adsorption on activated carbon of p-nitrophenol from aqueous solution. *Water research*, *23*(1), 85-91, 1989.

[29] DANISH, M., ANSARI, K. B., DANISH, M., KHATOON, A., RAO, R. A. K., ZAIDI, S., & AFTAB, R. A. , 2022. A comprehensive investigation of external mass transfer and intraparticle diffusion for batch and continuous adsorption of heavy metals using pore volume and surface diffusion model. *Separation and Purification Technology*, *292*, 120996.

[30] DORADO, A. D., GAMISANS, X., VALDERRAMA, C., SOLÉ, M., LAO, C., Cr (III) removal from aqueous solutions: a straightforward model approaching of the adsorption in a fixed-bed column. *Journal of Environmental Science and Health, Part A*, *49*(2), 179-186, 2014.

[31] SCHEUFELE, F.B., A.N. MÓDENES,C.E. BORBA, RIBEIRO, C. ESPINOZA-QUIÑONES, F.R. BERGAMASCO, R. N. PEREIRA, C. Monolayer–multilayer adsorption phenomenological model: kinetics, equilibrium and thermodynamics, *Chem. Eng. J.*, 284,1328–1341, 2016.

[32] JARIA, G., CALISTO, V., SILVA, C.P., GIL, M.V., OTERO, M., ESTEVES, V.I., Fixed-bed performance of a waste-derived granular activated carbon for the removal of micropollutants from municipal wastewater, *Sci. Total Environ,* 683, 699-708., 2019. https://doi.org/10.1016/j.scitotenv.2019.05.198.

[33] LI, H., HE, J., CHEN, K., SHI, Z., LI, M., GUO, P., WU, L., Dynamic adsorption of sulfamethoxazole from aqueous solution by lignite activated coke, *Materials 13*, 1785, 2020. https://doi.org/10.3390/ma13071785.

[34] JUELA, D., VERA, M., CRUZAT, C., ALVAREZ, X., VANEGAS, E., Mathematical modeling and numerical simulation of sulfamethoxazole adsorption onto sugarcane bagasse in a fixed-bed column. *Chemosphere*, *280*, 130687, 2021. https://doi.org/10.1016/j.chemosphere.2021.130687.

[35] YAMAMOTO, Y., YAJIMA, T., & KAWAJIRI, Y., Uncertainty Quantification for Chromatography Model Parameters by Bayesian Inference using Sequential Monte Carlo Method, *Chemical Engineering Research and Design*, 2021.

[36] DAS, L., SENGUPTA, S., DAS, P., BHOWAL, A., BHATTACHARJEE, C. Experimental and Numerical modeling on dye adsorption using pyrolyzed mesoporous biochar in Batch and fixed-bed column reactor: Isotherm, Thermodynamics, Mass transfer, Kinetic analysis. *Surfaces and Interfaces*, v. 23, p. 100985.

[37] IHEANACHO, O. C., NWABANNE, J. T., OBI, C. C., ONU, C. E. Packed bed column adsorption of phenol onto corn cob activated carbon: linear and nonlinear kinetics modeling. South African *Journal of Chemical Engineering*, v. 36, p. 80-93, 2021.

[38] MÓDENES, A. N., BAZARIN, G., BORBA, C. E., LOCATELLI, P. P. P., BORSATO, F. P., PAGNO, V., SCHEUFELE, F. B. Tetracycline adsorption by tilapia fish bone-based biochar: Mass transfer assessment and fixed-bed data prediction by hybrid statistical-phenomenological modeling. *Journal of Cleaner Production*, v. 279, p. 123775, 2021. https://doi.org/10.1016/j.jclepro.2020.123775.

[39] FEIZI, F., SARMAH, A. K., RANGSIVEK, R. Adsorption of pharmaceuticals in a fixed-bed column using tyre-based activated carbon: Experimental investigations and numerical modelling. *Journal of Hazardous Materials*, v. 417, p. 126010, 2021.

[40] ÖZIŞIK, M. N., ORLANDE, H. R., COLACO, M. J., Cotta, R. M. *Finite difference methods in heat transfer*. CRC press, 2017. https://doi.org/10.1201/9781315121475.

[41] KAIPIO, J., SOMERSALO, E., *Statistical and Computational Inverse Problems*, Springer, New York, NY, 2004. https://doi.org/10.1007/b138659.

[42] MOURA, C. H.R., VIEGAS, B. M., TAVARES, M., MACEDO, E., & ESTUMANO, D. C., (2022). Estimation Of Parameters And Selection Of Models Applied To Population Balance Dynamics Via Approximate Bayesian Computational. *Journal of Heat and Mass Transfer Research*. 10.22075/JHMTR.2022.25186.1361.

[43] PASQUALETTE, M.A., ESTUMANO, D.C., HAMILTON, F.C. . Bayesian estimate of pre-mixed and diffusive rate of heat release phases in marine diesel engines. *J Braz. Soc. Mech. Sci. Eng.* 39**,** 1835–1844, 2017. http://dx.doi.org/10.1007/s40430-016-0649-9.

[44] VIEGAS, B. M., MAGALHÃES, E. M., ORLANDE, H. R. B., ESTUMANO, D. C., & MACÊDO, E. N. (2022). Experimental study and mathematical modelling of red mud leaching: application of Bayesian techniques. *International Journal of Environmental Science and Technology*, 1-14. https://doi.org/10.1007/s13762-022-04346-x

[45] AMADOR, I.C.B., NUNES, K.G.P., DE FRANCO, M.A.E., VIEGAS, B.M., MACÊDO, E.N., FÉRIS, L.A., ESTUMANO, D.C., Application of Approximate Bayesian Computational Technique To Characterize The Breakthrough Of Paracetamol Adsorption in Fixed Bed Column, *International Communication in Heat and Mass Transfer*, 132 (2022) 105917, https://doi.org/10.1016/j.icheatmasstransfer.2022.105917.

[46] ESTUMANO, D.C., HAMILTON, F.C., COLAÇO, M.J., LEIROZ, A.J., ORLANDE, H.R., CARVALHO, R.N., & DULIKRAVICH, G.S. (2014). Bayesian estimate of mass fraction of burned fuel in internal combustion engines using pressure

measurements. *Engineering Optimization IV - Proceedings of the 4th International Conference on Engineering Optimization*, ENGOPT 2014, 2014, pp. 997–1004. http://dx.doi.org/10.1201/b17488-181.

[47] OLIVEIRA, R. F., NUNES, K. G. P., JURADO, I. V., AMADOR, I. C. B., ESTUMANO, D. C., & FÉRIS, L. A., Cr (VI) adsorption in batch and continuous scale: A mathematical and experimental approach for operational parameters prediction, *Environmental Technology & Innovation*, 20, 1092-1105, 2020. https://doi.org/10.1016/j.eti.2020.101092.

[48] MOURA C.H.R., VIEGAS B.M., TAVARES M.R.M., MACÊDO E.N., ESTUMANO D.C., QUARESMA J.N.N. Parameter estimation in population balance through Bayesian technique Markov Chain Monte Carlo, *J. Appl. Comput. Mech*., 7(2), 2021, 890–901. https://doi.org/10.22055/JACM.2021.35741.2725.

[49] NUNES, K. G. P., DÁVILA, I. V. J., AMADOR, I. C. B., ESTUMANO, D. C., & FÉRIS, L. A. (2021). Evaluation of zinc adsorption through batch and continuous scale applying Bayesian technique for estimate parameters and select model. *Journal of Environmental Science and Health, Part A*, 1-15. https://doi.org/10.1080/10934529.2021.1977059.

[50] NUNES, K. G. P., DAVILA, I. V. J., ARNOLD, D., MOURA, C. H. R., ESTUMANO, D. C., & FÉRIS, L. A. (2022). Kinetics and Thermodynamic Study of Laponite Application in Caffeine Removal by Adsorption. *Environmental Processes*, *9*(3), 47.

[51] GELMAN A, SIMPSON D, BETANCOURT M. The Prior Can Often Only Be Understood in the Context of the Likelihood, *Entropy*, 19(10), 555, 2017. https://doi.org/10.3390/e19100555.